Dielectric, thermal and optical properties of a metal-organic coordinated pyridinium complex

A. Philominal[1], S. Dhanuskodi[1*] and J. Philip[2]

[1]*School of Physics, Bharathidasan University, Tiruchirappalli, India*
[2]*Sophisticated Test and Instrumentation Centre, Cochin University of Science and Technology, Cochin, India*
_____

ABSTRACT

1-ethyl-2, 6-dimethyl-4 hydroxy pyridinium magnesium sulphate tetra hydrate (EDMPMS) has been synthesized and the single crystals were grown by slow evaporation technique. The grown crystals were characterized by elemental analysis, FTIR and FT NMR techniques to confirm the formation of the compound. Thermal stability has been investigated by TG/DTA, DSC and the melting point is 113 °C. The optical transmittance window in MeOH solution was found to be 262 - 800 nm by UV - Visible spectrocopy. The second order nonlinear optical property was studied by Kurtz-Perry technique. Impedance and dielectric measurements were performed for the frequency range 42 Hz – 5 MHz at 303 K.
_____

INTRODUCTION

Second order nonlinear optical materials have attracted much attention because of their potential applications in emerging optoelectronic technologies [1-2]. The common wisdom has been that an optical material should have a large charge transfer and optical transparency with less dislocation density [3]. A nonlinear optical (NLO) response in organic materials is microscopic in origin due to the presence of delocalized π-electron systems connecting donor and acceptor groups which are responsible for enhancing their asymmetric polarizability [4]. Inorganic materials have excellent chemical and mechanical properties like high mechanical strength, high melting point and high degree of chemical inertness but often these are limited in use because of low nonlinear optical coefficients compared with organics [5]. Hence the association of organic moieties with inorganic residues has been proposed for second order nonlinear optical materials. The properties of the materials be modified and improved by the amalgamation of the appropriate blocks with desirable functionalities [6-7]. Pyridine molecule is capable of forming the stable metal complexes through co-ordination bonds. These complexes show ligand to metal charge transfer (LMCT) by an elecctron movement from ligand to metal and metal to ligand (MLCT) in addition to π-π^* conjugation. Metals with completely filled d^{10} shell (Zn, Cd and Hg) and half filled d^5 shell (Mg) configurations readily combine with pyridine resulting in stable compounds with high optical nonlinearity and physiochemical behavior. One such molecule is 1-ethyl-2, 6-dimethyl-4 (1H) pyridinone trihydrate (EDMP) which exhibits quadratic NLO properties, in particular second harmonic generation (SHG) down to the UV region [8-9]. In the present study, the design, synthesis and properties (spectral, optical, thermal and dielectric) of the substituted pyridine molecule EDMPMS are reported.

1

_____

MATERIALS AND METHODS

Synthesis and Crystal Growth
EDMPMS was prepared by the reaction of EDMP with $MgSO_4$ in the molar ratio 2:1 in double distilled water. The starting materials have been prepared following the synthetic route reported by Garratt [8]. The synthesized salt was further purified by the repeated recrystallization process in double distilled water. The solubility test was carried out and water was identified as the suitable solvent for the growth of good quality crystals. Single crystals of EDMPMS with the dimensions (10 x 2 x 2 mm^3) were harvested after a typical growth period of 7 days from the saturated solution at 30 °C by the slow evaporation of the solvent.

RESULTS AND DISCUSSION

Microanalysis
The percentage composition of the elements carbon, hydrogen and nitrogen present in the compounds were identified by CHN analysis. The observed and computed values of the percentage composition of elements C, H and N present in EDMPMS are 23.78 (24.90), 8.27 (7.20) & 3.11 (3.20) and for the parent compound EDMP are 52.23 (52.67), 10.61 (9.33) & 6.59 (6.82). Here the reduction in the percentage composition of EDMPMS over EDMP evidence that the formation of the new compound and agrees well with observed and computed (given in the paranthesis) values.

Spectral Analyses
NMR Spectroscopy
NMR spectroscopy was used to identify the proton and carbon configurations of the synthesized compounds. ^1H (300 MHz, D_2O, 300 K) and ^{13}C NMR (300 MHz, $CDCl_3$, 300 K) spectra were recorded using a JEOL Model GSX 400, Bruker FT NMR spectrometer. The chemical shift of ^{13}C and ^1H NMR of EDMPMS with EDMP are compared in **table 1**.

Table 1 Chemical shift (δ ppm) of ^{13}C and ^1H NMR of EDMPMS with EDMP.3H_2O

EDMP	EDMPMS*	Origin
^{13}C NMR		
179.542	177.751	C–O
153.353	152.248	C–CH_3
118.345	116.815	C–H olefinic
20.787, 14.959	19.412, 13,389	ethyl
^1H NMR		
1.20	1.15 (triplet)	CH_3 (ethyl)
2.35	2.29 (singlet)	CH_3 (methyl)
3.97	3.95 (quartet)	CH_2 (ethyl)
4.69	4.71	O–H
6.27	6.23 (singlet)	C–H

Table 2: Comparison of the characteristic vibrational frequencies of EDMPMS with EDMP

Wave number (cm^{-1})		Assignments
EDMP [9]	EDMPMS	
3390-3185	3404	υ (O–H) H-bonded
3000	-	υ (C–H)
1631	1630	υ (C=O)
1549	1550	υ (C–H), overtone
1525	1524	υ (C=C)
1455	1456	δ (C–H)
1375, 1338	1377, 1339	δ (C–H of CH_3)
1198, 1183	1182, 1109	υ (C–N) or ρ(C–H)
1034	1086	υ (C–N)
-	984	$υ_s$ (SO_4)
881, 848	869, 842	π (C–H)
697	729	π (C–H)
-	629	δ (O–H)
494	502	π (C=O)

υ - stretching, $υ_s$ - symmetric stretching, δ - bending deformation in plane,
ρ - rocking in plane, π - bending out of plane

2

_____

Fourier Transform Infrared Spectrocopy
Infrared spectrocopy is effectively used to identify the functional groups and to elucidate the molecular structure of the compound. FTIR spectrum of EDMPMS was recorded in the range 400 - 4000 cm^{-1} employing a JASCO 460 PLUS FTIR spectrometer following the KBr pellet technique at 300 K. The comparison of characteristic vibrational frequencies of EDMPMS with EDMP is given in **table 2**.

Thermal studies
Thermogravimetric and differential thermal analyses give information regarding phase transition, water of crystallization and different stages of decomposition of the crystal system [10]. TG/DTA (**Fig. 1**) analyses were performed using Seiko instruments thermal analyser in the temp range 28°- 800 °C at a heating rate of 20 °C/min in nitrogen atmosphere. DSC measurement was carried out using Mettler Toledo DSC 822^e differential scanning calorimeter in the temperature range 30° – 400 °C at a heating rate of 10 °C/min. The initial mass of the sample for the thermogravimetric analysis was 7.232 mg and the weight loss due to the water molecules was observed in the low temperature region and it is clealy indicated in the DSC curve (**Fig. 2**). Both DTA and DSC curves confirm the melting point (113 °C) of the material. An endothermic peak observed in the region 200° - 600 °C shows the decomposition of the sample. A peak at 717 °C gives the presence of magnesium in the compound whereas TGA shows a complete weight loss and the remaining percentage of weight observed at 800 °C was only 10 %.
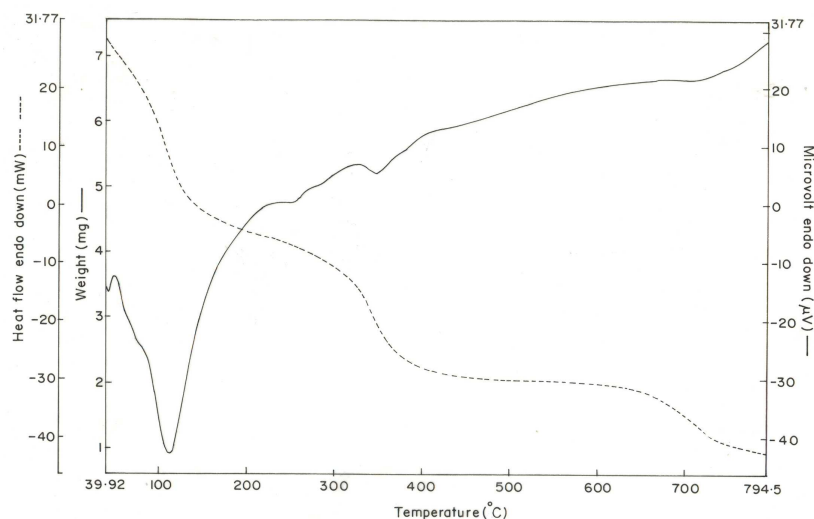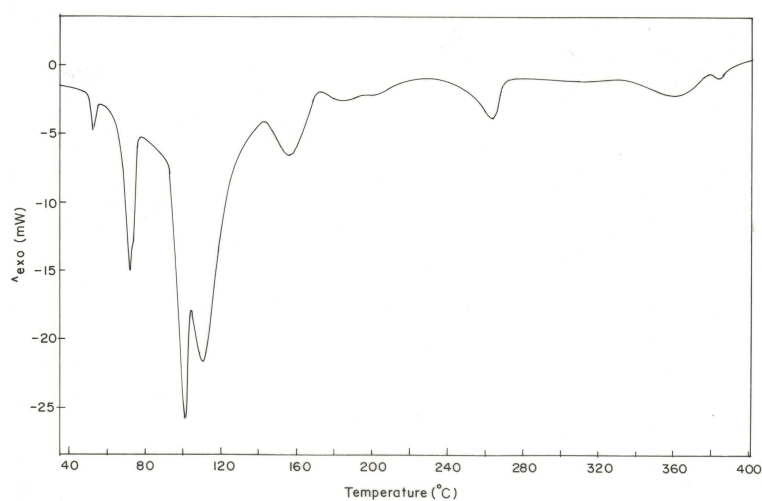

Fig. 1. TG/DTA curve of EDMPMS

Fig. 2. DSC curve of EDMPMS

_____

3.4. UV-Visible Spectrocopy

The optical absorption spectrum was recorded using a Varian Cary 5E UV-Vis spectrophotometer in the range 200-800 nm in MeOH (**Fig. 3**).
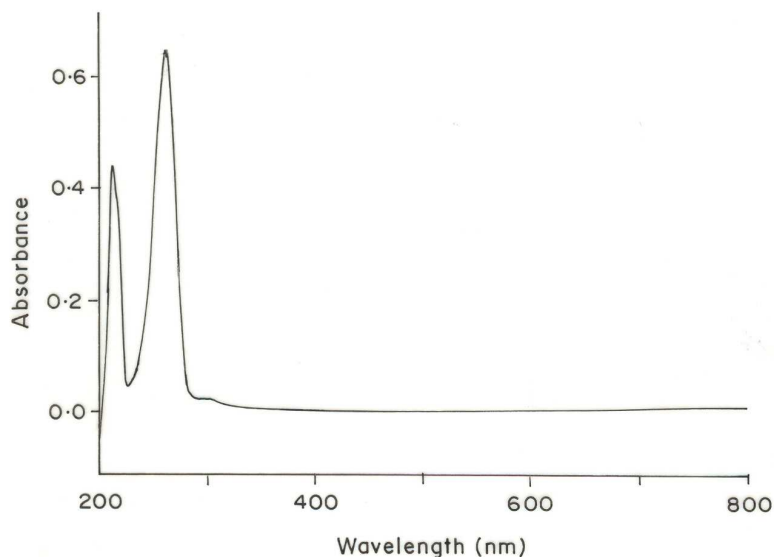

Fig. 3 UV absorption specturm

It is evident that the material has the UV absorption edge at 262 nm and good optical transmittance window covering the UV and visible region enables a promising candidate for the fabrication of nonlinear optical devices.
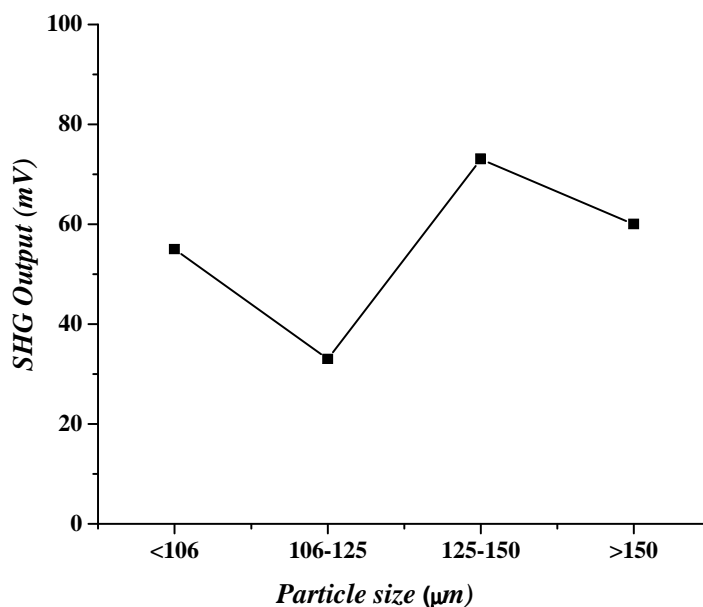

Fig. 4. SHG output vs particle size

3.5. Second Harmonic Generation Efficiency

Powder SHG measurements were carried out following the Kurtz-Perry technique [11] using a Q-switched Nd: YAG laser (1064 nm, 10 ns, 10 Hz, 3.3 mJ). All the crystalline powder samples were graded using standard sieves

4

A. Philominal *et al*   ***Arch. Appl. Sci. Res., 2013, 5 (4):1-7***

_____

with the particles size ranges (in μm) <106, 106-125, 125-150, and >150, and packed in a capilliary tubes of diameter 0.1 mm. The generated SHG signal from the randomly oriented crystallites was focussed at the slit of the monochromator and monitored by photomultiplier tube and cathode ray oscilloscope assembly. EDMPMS shows the SHG output 1.35 times of EDMP and 1.52 times that of KDP. The plot of SHG output vs particle size is shown in **Fig.4**. From the plot it is identified that, EDMPMS non-phase matchable.
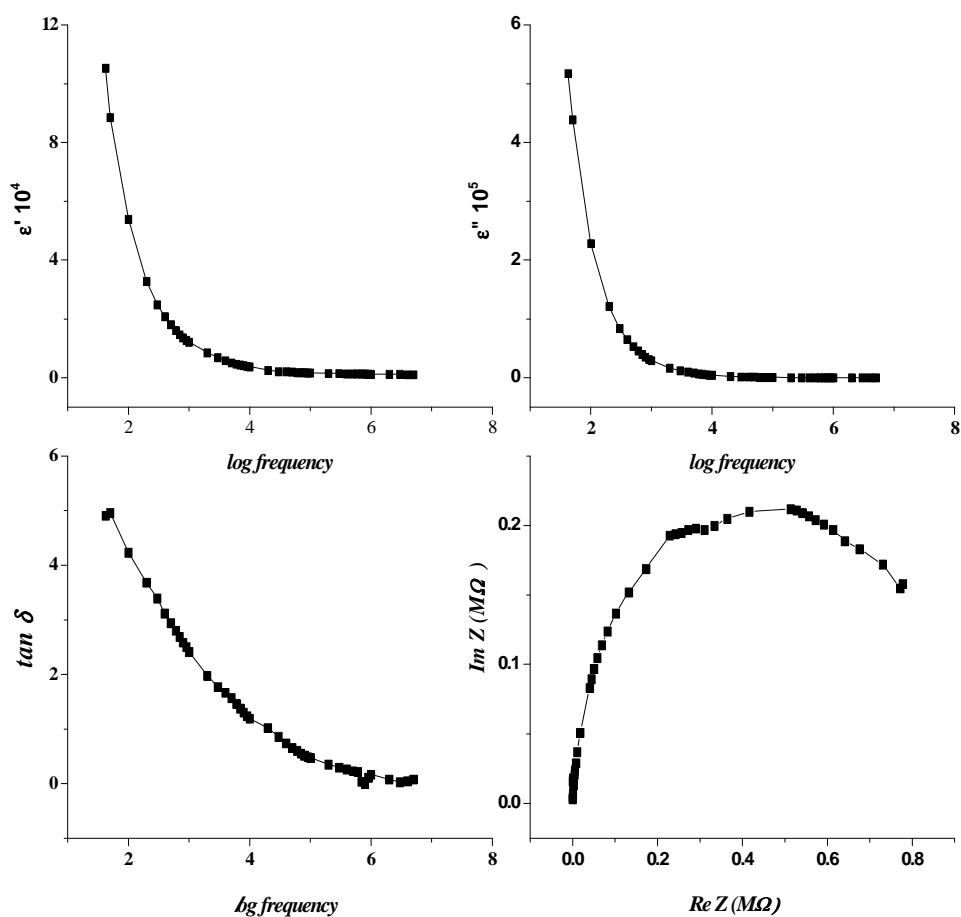

Fig. 5. Log frequency against *ε'* and *ε''*, tan δ and Re Z vs Im Z

3.6. Impedance spectroscopy

Impedance spectroscopy provides frequency resolved information which can detach the contributions of different component regions of the total electrical properties of devices through the differences in the time constants of each element [12-14].

Polycrystalline samples of EDMPMS were made in the form of pellets with a thickness of 1.3 mm and impedance measurements were carried out using a HIOKI LCR meter as a function of frequency (42 Hz – 5 MHz) at 303 K. The opposite flat faces were coated with conducting silver paint acting as the dielectric medium. The capacitance of the parallel plate capacitor (C), impedance (Z), phase angle (θ) and dissipation factor (tan δ) were measured.

The dielectric constant ε' and dielectric loss ε'' were calculated using the following relations

_____

$$\varepsilon' = \frac{Cd}{\varepsilon_0 A} \tag{1}$$

$$\varepsilon'' = \varepsilon' \tan \delta \tag{2}$$

Here C is the capacitance of the parallel plate capacitor (pF), d is the thickness of the crystal (mm), A is the area of the crystal acting as the dielectric, ε_o is the permittivity of free space (8.854 x10^{-12} F/m) and tan δ is the dissipation factor. Plots of ε' and ε'' against *log (frequency)* at 30 °C are shown in **Fig. 5.** The large value of dielectric constant at low frequency is attributed to the space charge polarizations.

Fig. 6 shows the variation of real (Z') and imaginary (Z'') parts of impedance with frequency at 30 °C. It can be seen that the curves display decrease in Z'with frequency. The Z'' values reach a maximum with frequency and shift to lower frequencies indicating a decrease in relaxation time in the system. The relaxation times were calculated from the frequency at which Z'' maxima are observed.
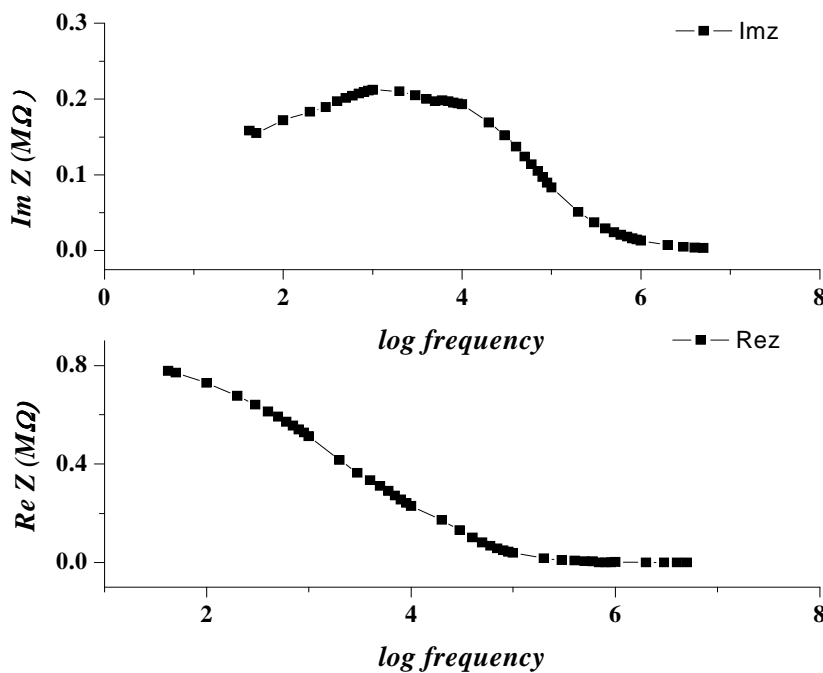

Fig. 6. Real (Z') and imaginary (Z'') parts of impedance with frequency

The theoretical values of real and imaginary components of an equivalent circuit were calculated using the relationships,

$$Z' = Rs + \frac{Rp}{1 + \omega^2 Co^2 Rp^2} \tag{3}$$

$$Z'' = \frac{\omega CpRp^2}{1 + \omega^2 Co^2 Rp^2} \tag{4}$$

Here the components of total capacitance are in parallel and this equivalent circuit has single time constant. Plots of Z'vs Z'' for the range of frequencies show semicircular nature indicating the predominance of a single time constant. To analyse and interpret experimental data, it is essential to have a equivalent circuit model that provides a realistic representation of the electrical properties.This is chosen based on (i) Intuition as to what kind of impedance is expected to be present in the sample and whether they are connected in series or in parallel. (ii) Examination of the experimental data to see whether the response is consistent with the proposed circuit. (iii) Inspection of the

6

_____

resistance and capacitance values that are obtained in order to check that they are realistic and that their temperature is reasonable with a series circuit.

Present studies were performed to understand the electrical properties by means of impedance spectroscopy, the frequency response of the material under an alternating current was studied. This work presents the impedance data in the complex impedance plane and can be represented by equivalent circuits which give essential inputs for device applications. The grain and grain boundary contributions have to be separated.

These complex impedance plots can be represented by the equivalent circuit models is shown in fig. Each semicircle is represented by a parallel resistance – capacitance circuit corresponding equivalent to the individual component of the materials ie. bulk or grain and grain boundary. The resistances of each element are directly obtained from the intercept on the X-axis. ie. Real part of the impedance. The capacitance can be calculated using the equation,

$\omega\tau = 1$ ie. $\omega RC=1$ (5)

Where ω is the maximum frequency of the semicircle for the component. At 303 K only one broad unresolved semicircle was observed and this was resolved into two semicircles intercepting each other on the X-axis. The high frequency semicircle represents the materials bulk electrical properties while the low frequency semicircle indicates the electrical behaviour of grain boundary.

CONCLUSION

A new second order nonlinear optical material was synthesized and single crystals were grown by slow evaporation technique. Micro analysis reveals that the formation of the compound by the presence of percentage composition of elements. Molecular structure was confirmed by FTIR and FT NMR spectra. Thermal stability of the compound was identified by TG/DTA and DSC. It does not show any decomposition before melting. Dielectric measurement reveals that both the dielectric constant and the dielectric loss decrease with increasing frequency. The real and imaginary part of the impedance for the range of frequencies show a semicircular nature indicating the occurrence of single time constant. The proposed equivalent circuit model gives the essential inputs for device applications.

REFERENCES

[1] Weiguo Zhang, Xutang Tao, Chengqian Zhang, Huaijin Zhang, Minhua Jiang, *Cryst Growth Des*., **2009**, 9, 2633-2636.
[2] S. Dinakaran, Sunilverma, C. Justin Raj, J. Mary Linet, S. Krishnan, S, Jerome Das, *Cryst, Growth Des*., **2009** 9, 151-157.
[3] A. Bhaskaran, C. M. Raghavan, R. Sankar, R. Mohankumar, R. Jayavel, *Cryst. Res. Technol*., **2007**, 42, 477-482.
[4] D. Balasubramanian, R. Sankar, V. Sivasankar, P. Murugakoothan, P. Arulmozhiselvan, R. Jayavel, *Mater. Chem. Phys*., **2008,** 107, 57-60.
[5] E. Y. Lee, S. Y. Jang, M. P. Suh, *J. Am. Chem. Soc*., **2005,** 127, 6374-6381.
[6] M. K. Marchewka, S. Debrus, H. Ratejczak, *Cryst. Growth Des*., **2003,** 3, 587-592.
[7] C. D. Wu, A. Hu, L. Zang, W. Lin, *J. Am. Chem. Soc.,* **2005**, 127, 8940-8941.
[8] S. Garratt, *J. Org. Chem*., **1963,** 28, 1886-1888.
[9] Manivannan, S.K. Tiwari, S. Dhanuskodi, *Solid State Commun*., **2004**, 132, 123-127.
[10] B. Milton Boaz, P. Santhana Raghavan, S. Xavier Jesu Raja, S. Jerome Das, *Mater. Chem. Phys*., **2005**, 93, 187 – 193.
[11] S. K. Kurtz, T. T. Perry, *J. Appl. Phys.,* **1968**, 39, 3798.
[12] R. A. Kumar, M. S. Suresh, J. Nagaraju, *Sol. Energy Mats. Sol. Cells*, **2000**, 60, 155.
[13] A. K. Jonscher, Dielectric Relaxation in Solids, Chelsea Dielectrics Press, London, **1983**.
[14] M. S. Suresh, *Sol. Energy Mats. Sol. Cells*, **1996**, 43, 21.